Vesicular glutamate transporter 3-immunoreactive pericellular baskets ensheath a distinct population of neurons in the lateral septum

Anett Riedel[a,b,*], **Sören Westerholz**[a,b], **Katharina Braun**[a,b], **Robert H. Edwards**[c,d], **Thomas Arendt**[e], and **Wolfgang Härtig**[e]

[a] Department of Zoology/Developmental Neurobiology, Otto von Guericke University, Magdeburg, Institute of Biology, Leipziger Str. 44, Haus 91, D-39120 Magdeburg, Germany

[b] Department of Physiology, Otto von Guericke University, Magdeburg, POB 1860, 39008 Magdeburg, Germany

[c] Department of Neurology, University of California at San Francisco School of Medicine, San Francisco, 94143 CA, United States

[d] Department of Physiology, University of California at San Francisco School of Medicine, San Francisco, 94143 CA, United States

[e] Paul Flechsig Institute for Brain Research, University of Leipzig, Jahnallee 59, D-04109 Leipzig, Germany

Abstract

The lateral septum (LS) plays a role in the adjustment of behavioral responses according to environmental demands. This is a complex integrative process wherein a variety of modulatory systems, i.e. cholinergic, dopaminergic and serotonergic projections forming pericellular baskets around LS neurons, are involved.

Recently, vesicular glutamate transporter 3 (VGLUT3)-immunoreactive (-ir) structures outlining unlabeled somata and their proximal dendrites were described in the LS. However, the vesicular transporters for acetylcholine and GABA were not or only rarely co-expressed with VGLUT3.

In this study, the morphology and distribution of these VGLUT3-ir structures were systematically analyzed revealing that (1) they form distinct pericellular baskets (PBs) displaying variable shapes, (2) they are arranged in a layer-like pattern similar to the terminals of other modulatory systems, (3) beside a few exceptions (e.g., choline acetyltransferase), they are generally not or very sparsely co-localized with other neurochemical markers characterizing major neuron populations or afferent systems of the LS, i.e. calcium-binding proteins, tyrosine hydroxylase, tryptophan hydroxylase, vesicular glutamate transporters 1 (VGLUT1) and 2 (VGLUT2) and the vesicular GABA transporter.

Thus, in the LS, a separate population of neurons is covered by VGLUT3-ir PBs. The distribution pattern and the lack of co-localization indicate that the VGLUT3-expressing cells of origin are located in the brainstem and that they could be pure glutamatergic projection neurons–different from the well-defined canonical VGLUT1- and VGLUT2-expressing neurons. Alternatively, they could

simultaneously express VGLUT3 and second transmitter, but use different release sites inside the LS for both.

1. Introduction

The lateral septum (LS) plays an essential role in the integration of cognitive, emotional and autonomous processes. Thereby, it is involved in the control of affective and motivational behavior, in the regulation of fear and anxiety and in the development of drug abuse (Sheehan et al., 2004). The diversity of integrative operations conducted by the LS is reflected by its central location inside the brain and by its extensive, predominantly reciprocal connections with various brain regions extending from the telencephalon down to the spinal cord (Risold, 2004). The intrinsic organization of the LS is highly complex. It consists of a variety of morphologically and neurochemically characterized cell populations, which tend to be arranged in a lamina-like pattern, thereby ignoring the borders of the major three nuclei and further dividing them into subregions. The ascending axons from deeper brain areas, e.g., dopaminergic, cholinergic, serotonergic and several peptidergic afferents form distinct pericellular formations, called pericellular baskets, inside the LS. In general, their termination pattern also displays a layerlike arrangement (Jakab and Leranth, 1995; Risold and Swanson, 1997a,b).

Recently, VGLUT3-immunoreactivity (VGLUT3-ir) structures outlining unlabeled cell somata and their proximal dendrites were described in the LS on cells that were not otherwise characterized (Herzog et al., 2004). The VGLUT3 belongs to the type I phosphate transporter family; and in contrast to VGLUT1 and VGLUT2 it is usually not found in canonical asymmetric glutamatergic synapses, but rather localizes to non-glutamatergic serotonergic, cholinergic or GABAergic neurons and to a small subset of astrocytes (Fremeau et al., 2004; Seal and Edwards, 2006). In the basal forebrain, axonal co-expression of VGLUT3-immunoreactivity was shown for the striatal cholinergic interneurons. In contrast, the VGLUT3-ir fibrous structures in the LS did not co-express acetylcholine, serotonin and, only rarely, GABA (Fremeau et al., 2002; Gras et al., 2002; Herzog et al., 2004).

Despite the apparent VGLUT3-ir PBs, VGLUT3-mRNA was not expressed in LS neurons in all these studies; a finding that was recently confirmed by Geisler et al. (2007). In contrast, VGLUT3-mRNA was found in deeper brain areas like hypothalamus, substantia nigra and dorsal raphe (Fremeau et al., 2002; Gras et al., 2002; Herzog et al., 2004; Schäfer et al., 2002). Projection neurons located in these regions innervate the LS and their terminals form perisomatic and peridendritic plexus called pericellular baskets (Jakab and Leranth, 1995).

The aim of this study was to analyze whether the VGLUT3-ir structures in the LS form distinct PBs displaying a defined distribution pattern. Secondly, we wanted to reveal co-localization and the spatial relationship of the VGLUT3-ir PBs with well-defined neuron subpopulations and/or the fiber systems projecting to and passing the LS. Thus, we performed single and double immunofluorescence staining of VGLUT3 and the calcium-binding proteins calbindin (CALB), calretinin (CALR) and parvalbumin (PARV), with choline acetyltransferase (ChAT), tyrosine hydroxylase (TH) and tryptophan hydroxylase (TrpH), and with *Wisteria floribunda* agglutinin (WFA) revealing perineuronal nets (Bialowas and Frotscher, 1987; Gall and Moore, 1984; Jacobowitz and Winsky, 1991; Kiss et al., 1997; Seeger et al., 1994; Seifert et al.,

1998). Triple labeling of VGLUT3 with VGLUT1 and VGLUT2 was performed, as the LS is known to be positive for both glutamatergic markers and it was recently suggested, that projection neurons in the intermediate and ventral LS use glutamate as neurotransmitter (Kaneko et al., 2002; Kocsis et al., 2003; Lin et al., 2003). Finally, we investigated the relationship of VGLUT3-ir and the vesicular GABA transporter (VGAT)–which heavily labels the entire septum (McIntire et al., 1997).

2. Materials and methods

2.1. Animals, perfusion and sectioning

Twelve 4-month-old male and female Wistar rats were used for this study. All experiments were performed in accordance with the European Communities Council Directive (86/609/EEC) and the German guidelines for the care and use of animals in laboratory research. The animals were deeply anaesthetized with pentobarbital and perfused with ice-cold saline. Afterwards, animals were perfused with a fixation solution made of 4% paraformaldehyde and 0.1% glutaraldehyde dissolved in 0.1 M phosphate buffer (PB; pH 7.4). Then, brains were removed from the skulls and post-fixed in the same solution which was used for perfusion fixation (overnight at 4 °C). Prior to sectioning, the tissue was cryoprotected in 30% sucrose in PB until equilibration. In the beginning, LS sections of two rats were used for pilot experiments including the neuronal counterstaining (Table 1, experiment 1). For the analysis of VGLUT3-ir, eight brains were used as follows: 10 series of 30-μm-thick frontal sections starting at the most rostral level (Bregma +1.70 mm according to Paxinos and Watson, 1998) and reaching to the most caudal level of the LS (Bregma −0.40 mm) were cut with a freezing microtome (Leica, Bensheim, Germany) and collected in Tris-buffered saline (TBS; 0.1 M, pH 7.4). The first series was always single stained for VGLUT3 (Table 1, experiment 2). Other series were subsequently stained with the different marker combinations according to Table 1 (experiments 3–10) and *W. floribunda* agglutinin (WFA). Moreover, series of horizontal sections (Bregma −6.38 to −3.86 mm) from two animals were prepared. The horizontal sections were either single stained for VGLUT3-ir or double stained for VGLUT3- and TH-ir.

2.2. Characterization of antibodies

The primary antibodies used in the present study are listed in Table 1, which also includes the host species, immunogens, applied dilutions and the source. The primary antibodies were characterized as follows: Initially, the specificity of the guinea pig anti-VGLUT3 antiserum was checked by comparing the staining patterns with those of rabbit anti-VGLUT3 antiserum yielding to identical results not only in the LS, but also in other regions (e.g., striatum, cortex). Pre-adsorption experiments of both VGLUT3 antisera with the corresponding glutathione-*S*-transferase-conjugated fusion protein used for the generation of both antibodies resulted in the absence of any staining (Harkany et al., 2003). For the detection of neuronal nuclei (NeuN) we used a well-defined specific monoclonal antibody (Mullen et al., 1992). Antibodies directed against the calcium-binding proteins were characterized by Celio's group. Thus, immunoblotting elucidated single protein bands of 12, 28 or 29 kDa recognized by mouse anti-PARV (Celio et al., 1988), mouse anti-CALB (Celio et al., 1990) and rabbit anti-CALR (Schwaller et al., 1993), respectively. Western blotting with rabbit anti-TH revealed a single protein band of about 60 kDa, whereas sheep anti-TrpH exclusively recognized a band of approximately 55 kDa (Chemicon/Millipore). The specificity of affinity-purified goat anti-ChAT was shown by abolishing the immunolabeling after antibody pre-incubation with ChAT protein (Li and Furness, 1998). Montana et al. (2004) and Synaptic Systems as manufacturer provided adsorption controls, in which the binding of mouse anti-VGLUT1 and rabbit anti-VGLUT2 was prevented.

2.3. Single and multiple immunofluorescence labeling

These staining procedures were started by blocking non-specific binding sites in TBS containing 5% normal donkey serum for 1 h. For single fluorescence labeling, the sections were solely incubated with guinea pig anti-VGLUT3 antiserum (1:300). All subsequent steps for the visualization of VGLUT3-ir were performed as described for the double staining experiments (section below).

For double fluorescence labeling, the sections were incubated with mixtures of guinea pig anti-VGLUT3 antibody and a second marker (experiments according to Table 1) in the blocking solution overnight. Rinsed sections were then incubated with mixtures of carbocyanine (Cy) 3-conjugated donkey anti-guinea pig and Cy2-tagged donkey antibodies directed against mouse, rabbit or goat (cross-reacting with sheep) according to the host species of primary antibody. All secondary antibodies applied were obtained from Dianova (Hamburg, Germany as supplier for Jackson ImmunoResearch, West Grove, PA) and used at 20 μg/ml in TBS containing 2% bovine serum albumin (BSA) for 1 h at room temperature.

For triple fluorescence staining, sections were simultaneously incubated with guinea pig anti-VGLUT3, goat anti-ChAT and mouse anti-VGLUT1 and detected with Cy3-tagged donkey anti-guinea pig, Cy2-coupled donkey anti-goat and Cy5-conjugated donkey anti-mouse (experiment 4 according to Table 1). Furthermore, sections were labeled with guinea pig anti-VGLUT3, mouse anti-PARV, and rabbit anti-VGLUT2 which were visualized with Cy3-tagged donkey anti-guinea pig, Cy2-coupled donkey anti-mouse and Cy5-conjugated donkey anti-rabbit (experiment 5 according to Table 1). Finally, vesicular glutamate transporters were triple-labeled by incubating the sections with a mixture of guinea pig anti-VGLUT3, rabbit anti-VGLUT2 and mouse anti-VGLUT1 detected with Cy3-tagged donkey anti-guinea pig, Cy2-coupled donkey anti-rabbit and Cy5-conjugated donkey anti-mouse (experiment 8 according to Table 1).

Additionally, the Cy3-immunodetection of VGLUT3 was combined with a lectin-histochemical staining based on biotinylated WFA (20 μg/ml) labeling perineuronal nets (Härtig et al., 1992) which was visualized with Cy2-streptavidin. All sections were carefully rinsed, mounted onto fluorescence-free glass slides, air-dried and coverslipped with Entellan (Merck, Darmstadt, Germany).

In control experiments, the omission of primary antibodies resulted in the absence of any cellular labeling. Additional controls were performed by switching the fluorochromated secondary antibodies in the double and triple labeling procedures which resulted in identical staining patterns.

2.4. Microscopy and figure production

Fluorescence sections were examined with an Axio Imager.Z1 microscope equipped with an AxioCamHRc for digital photomicroscopy and the appropriate band-pass (BP) filters and beam splitters (BS; all components from Zeiss, Germany). Hence, Cy2-fluorescence was checked with filter set no. 13 (excitation: BP 470/20 nm; BS 495 nm; emission: BP 503–530 nm, i.e. green color). Cy3-fluorescence was checked with filter set no. 43 (excitation: BP 545/25 nm; BS 570 nm; emission: BP 605/70 nm, i.e. red color). Double labeling was checked with filter set no. 24 (excitation: double BP 485/20 + 578/14 nm; double BP 500 + 600 nm; emission: BP 515–540 nm + LP 610 nm, i.e. yellow color). Further on, sections were analyzed with the LSM 510 Meta (Zeiss) equipped with an argon laser (488 nm) for the excitation of Cy2 and two helium–neon lasers (543 nm for the excitation of Cy3; 633 nm for excitation of Cy5). The following band-pass filters were used for the detection of the emission spectra–Cy2: BP500–530 nm (green color); Cy3: BP565–615 nm (red color); Cy5: BP 654–718 (red color re-coded

to blue). Hence, in single planes, yellow color (Cy2 and Cy3), magenta (Cy3 and Cy5) and turquoise (Cy2 and Cy5) means co-localization. All confocal images (Figs. 4 and 5) except Fig. 4A (single plane) are *z*-stack projections, single planes have been checked before stacking according to co-localization of markers.

Figs. 1 and 3 (and Supplementary figure) are montages of single images from one section. Original images were taken using the 200-fold magnification with Axio Vision 4.6 software (Zeiss) and compiled with Adobe Photoshop 7.0 (Adobe Systems Inc., Mountain View, CA). Brightness, contrast and sharpness of the final montages were slightly enhanced. Confocal images (Figs. 4 and 5) were scanned and edited using LSM Meta software (Zeiss).

3. Results

3.1. Regional distribution of VGLUT3-ir inside the LS

VGLUT3-ir dots were either loosely scattered or appeared as pericellular baskets in both male and female rats (Figs. 1 and 2). These VGLUT3-ir profiles did not match the borders of the dorsal (LSD), intermediate (LSI) and ventral (LSV) lateral septal subnuclei. The VGLUT3-ir PBs showed a layer-like distribution throughout the entire rostrocaudal extent of the LS. Most rostrally, where the indusium griseum extends far ventrally, few large VGLUT3-ir PBs were scattered in dorsal and lateral parts of the LSI (Fig. 1A). Further caudally, at the level of the rostral tip of the medial septum (MS), a curved stripe of VGLUT3-ir PBs extended from the LSD to the medial LSI, whereas the mediolateral LSI and the LSV were nearly devoid of them (Fig. 1B). At intermediate levels of the LS a prominent cluster of VGLUT3-ir PBs was appreciable in the LSD extending into the lateral LSI along the medial wall of the lateral ventricle (Fig. 1C). A very thin rim of VGLUT3-ir PBs accumulated at the border between the MS and the LSI. Parallel to this narrow zone, a prominent oblique band of VGLUT3-ir PBs was visible along the entire dorsoventral extent of the medial LSI whereas the mediolateral LSI was devoid of VGLUT3-ir PBs (Fig. 1C). In more caudal sections, where the rostral tip of the bed nucleus of the stria terminalis (BST) emerges, the prominent band of VGLUT3-ir PBs covering the medial LSI was still obvious. In contrast, the narrow rim of VGLUT3-ir PBs along the border to the MS was not any longer visible (Fig. 1D). At this level, the LSD was densely populated with VGLUT3-ir PBs. This cluster extended into the LSI along the medial wall of the lateral ventricle similar to the more rostral levels (Fig. 1C and D) where the LSV displayed a homogeneous VGLUT3-ir fiber meshwork (Fig. 1D). At most caudal levels of the LS, where the anterior commissure crosses the midline, VGLUT3-ir terminals did not form as distinct PBs, but were still clustered. Accumulations of VGLUT3-ir terminals were detectable in the medial LSD, medial and ventrolateral LSI and within the septofimbrial nucleus (Fig. 1E). The latter became obvious in VGLUT3/CALB double-stained sections where the nucleus septofimbrialis (VGLUT3-ir, CALB-negative) is located laterally to the nucleus triangularis septi (VGLUT3-negative, CALB-positive; not shown). The caudal LSV displayed an inhomogeneous VGLUT3-ir fiber meshwork with highest densities in its lateral part and a narrow stripe bordering the BST (Fig. 1E). In horizontal sections, the pattern of oblique stripes of VGLUT3-ir PBs was also nicely appreciable. Thus, the LSD showed a prominent cluster, a broad band reaching from rostromedial to caudolateral was visible in the LSI and the LSV was most densely populated with VGLUT3-ir PBs in its caudal portions (Fig. 1F).

3.2. Appearance of VGLUT3-ir PBs and morphology of cells outlined

VGLUT3-ir PBs were attached to NeuN-ir cell somata indicating that these cells are neurons (Fig. 2A/A′). VGLUT3-ir fibers characterized by prominent VGLUT3-ir dots were outlining cells, thereby forming pericellular baskets. The appearance of these PBs was not uniform as the VGLUT3-ir punctate staining showed differences in intensity and distinctness around single cells (Fig. 2B–E). The cells covered with VGLUT3-ir PBs appeared multipolar,

triangular, bipolar or round. Number and arrangement of labeled primary and secondary dendrites differed remarkably. Up to five primary dendrites were visible in our preparations and frequently the first branching could be detected. Morphology and orientation of each PB seemed to be unique (Fig. 2A–E). In most caudal sections, the VGLUT3-ir PBs were not as distinct or even absent. Areas with PBs contained additional VGLUT3–ir dots that also tended to form beaded fiber-like structures traversing the respective areas without an obvious system (Fig. 2B–E). In LS regions devoid of VGLUT3-ir PBs, VGLUT3-ir dots were less frequent, widely scattered, and not forming fiber-like structures within the sections. In horizontal sections, the appearance of VGLUT3-ir PBs was similar.

3.3. Co-existence of VGLUT3-ir PBs with markers of special neuron populations and afferents

3.3.1. Calbindin—The few scattered CALB-ir cells in the rostral LS, LSD and medial LSI were intermingled with VGLUT3-ir baskets (Fig. 3A/A′). A minority of these CALB-ir cells was outlined with VGLUT3-ir PBs (Fig. 4A). In the mediolateral or central LSI harboring the major clusters of CALB-ir somatospiny neurons, VGLUT3-ir fibers or PBs were only scarcely found (Fig. 3A/A′). Both markers were not co-expressed on single cells in this subnucleus. In the subventricular zone of the LSI, CALB-ir neurons intermingled with and were sometimes covered by loosely scattered VGLUT3-ir fibers and punctate (Fig. 4B). At caudal levels, the densely arranged CALB-ir cells in the lateral LSI and LSV were embedded in dense meshwork of VGLUT3-ir terminals which did not appear as distinct PBs. In general, both markers were not co-localized in the caudal LS, but VGLUT3-ir punctate sometimes attached to CALB-ir cells similar to the rostral or subventricular regions.

3.3.2. Calretinin—In the rostral LS, the CALR-ir cells assembled along the medial wall of the lateral ventricle. In this cluster, no VGLUT3-ir baskets and only very few fibers were found. Few CALR-ir neurons were observed in the rostral subcallosal LS where the most rostral VGLUT3-ir PBs were detected, however, they were not co-localized. At intermediate levels of the LS, CALR-ir cells accumulated additionally in the border region of LSI and MS. The dorsorostral portion of these CALR-ir cells (lambdoid septal zone according to Paxinos et al., 1998; Bregma 0.641) intermingled with the most medial cluster of VGLUT3-ir PBs. The ventrocaudal and major portion of this CALR-ir cell cluster (layer III according to Jakab and Leranth, 1995) was located medially to the assembly of VGLUT3-ir PBs. In contrast, few VGLUT3-ir PBs and fibers were intermingled with the clusters of CALR-ir cells in the LSV where no co-labeling was found. In the intermediate and caudal LSD, beside a few CALR-ir cells, a prominent fibrous CALR-ir labeling was obvious. Inside this CALR-ir fiber meshwork pericellular arrangements were visible; however, these did only occasionally co-express VGLUT3-ir (Fig. 4C).

3.3.3. Parvalbumin—PARV-ir cells in the LS were found only rarely in the subcallosal region of LSD. Labeling of these cells did not coincide with that of VGLUT3-ir baskets. Additionally, we observed PARV-ir in a small stripe of the intermediate LS region bordering the MS (Kiss et al., 1997). In this border region, PARV-labeled beaded fibers were visible, sometimes forming pericellular basket-like structures. These PARV-ir fibers and PBs were not co-labeled with VGLUT3-ir (Fig. 4D).

3.3.4. ChAT—In the LS, very few ChAT-ir cells were found in the medial and lateral LSI as well as in the LSV throughout the rostrocaudal extent (0–3 per section). About half of this small population of cells appeared completely VGLUT3-negative. The other ChAT-ir cells were VGLUT3-positive and displayed a rather homogeneous staining of the perikarya and primary dendrites similar to the cholinergic cells in the striatum (Fig. 4E). In the subcallosal LSD, fine cholinergic fibers were labeled; these fibers even formed pericellular baskets in the septohippocampal nucleus and medial LSD. However, the cholinergic fibers were never co-

labeled with VGLUT3-ir although both types of fibers were intermingled in these dorsal septal regions (Fig. 4F).

3.3.5. Tyrosine hydroxylase—Compared to the other markers, the lamina-like distribution of TH-ir fibers showed a stronger overlap with the layers and clusters of VGLUT3-ir PBs (Fig. 3B/B′). Thus, in the LSD, medial and subventricular LSI, and less dense in the LSV, TH-ir and PB-ir fibers were intermingled, and formed separate pericellular arrangements differing in their morphology. Fine and smooth TH-ir fibers enwrapped the somata and primary dendrites of LS cells, whereas the VGLUT3-ir terminals displayed a distinct and prominent punctate staining (Fig. 5A and B). Most of the VGLUT3-ir PBs intermingling with the TH-ir fiber network were completely single labeled. However, there was a small subpopulation of VGLUT3-ir PBs in the medial LSI that attached to the same cells as TH-ir fibers, but did not co-localize (Fig. 5A and B).

3.3.6. Tryptophan hydroxylase—TrpH-ir fibers were arranged in the typical layer-like pattern. They were loosely found in the rostral LSD forming pericellular arrangements which intermingled with VGLUT3-ir baskets but did not co-localize with them. At the intermediate level of the LS, the cluster of TrpH-ir fibers formed a subventricular layer where VGLUT3- and TrpH-ir overlapped, but were not co-expressed. Additionally, a small cluster of TrpH-ir fibers was found in the medial LSI bordering the MS where the VGLUT3-ir PBs of the MS–LS border regions were partly intermingled. This TrpH-ir fiber cluster is the rostral tip of the semicircular layer that appears prominent in more caudal regions of LSI crossing it from dorsomedial to ventromedial lateral to the fornical fibers. Caudally, the VGLUT3-ir fiber cluster was situated lateral to the TrpH-ir semicircular layer (Fig. 3C/C′). At the most caudal levels, the ventral ends of the subventricular and semicircular TrpH-ir layers merge in the caudal LSI and LSV where VGLUT3-ir fibers and PBs showed strong overlap, but no co-localization with TrpH-ir. Attachment of TrpH- and VGLUT3-ir fibers to the same cell was not found (Fig. 5C).

3.3.7. WFA—At rostral and intermediate LS levels, WFA-binding perineuronal nets (PNs) were only rarely found but they were numerous in the LSD. Moreover, clusters of WFA-decorated PNs formed an onion skin-like band in the caudal LS (Fig. 3D/D′). The staining pattern of PNs is different from that of the VGLUT3-ir PBs. In WFA-stained sections, the somata and primary dendrites of single cells are outlined by very fine punctate forming rather grid-like coatings (Fig. 5D). However, we noticed that the PNs were less intensely stained in the LS than, e.g., in different neocortical areas; namely only proximal dendritic processes were partly revealed. The distribution of WFA-binding PNs overlapped with that of VGLUT3-ir PBs. However, there were only a few cells outlined by VGLUT3-ir terminals which were additionally coated with WFA-binding PNs (Fig. 5D).

3.3.8. VGLUT1 and VGLUT2—In sections monolabeled for VGLUT1, the neuropil in the LS was homogeneously stained with a density similar to the dorsal striatum. In contrast, the MS could be sharply segregated by a very low VGLUT1-ir. Similarly, the Islands of Calleja and the ventral as well as dorsal pallidum displayed a very weak VGLUT1-ir, they are thereby sharply delineated from their neighboring regions (not shown). VGLUT2-ir did not label the LS in such uniform manner. The rostral LS can be delineated from the dorsal peduncular cortex by a more intense, but relatively homogeneous fiber staining. More caudally, the VGLUT2-stained fibers started to form pericellular arrangements in the LSD and medial and dorsal subventricular LSI but not in the LSV where they formed a dense meshwork. However, these pericellular arrangements were not as distinct as the VGLUT3-ir PBs, but became very prominent at intermediate LS levels where they omitted only the central LSI and the LSV. Nearly the entire caudal LS was populated with VGLUT2-ir PBs except its ventral regions.

Triple fluorescence labeling of vesicular glutamate transporters revealed that in all LS subnuclei VGLUT1- and VGLUT2-ir was infrequently co-expressed in single VGLUT3-ir terminals (Fig. 5E).

In the LSV the three markers are even more segregated, VGLUT3/VGLUT1-co-labeling and VGLUT3/VGLUT2-labeling occur only exceptionally.

3.3.9. VGAT—VGAT-staining uniformly labels the entire LS and, thus, is present in all subregions characterized by VGLUT3-ir. Confocal scans revealed that co-localization of VGAT inside VGLUT3-ir PBs was only rarely found in the LSD, but not at all in the LSI and LSV (Fig. 5F).

4. Discussion

4.1. Distribution of VGLUT3-ir throughout the lateral septum

Here we describe for the first time that distinct VGLUT3-ir PBs are found throughout the entire rostrocaudal extent of the lateral septum. These VGLUT3-ir PBs in the LS are very prominent, characterized by a typical punctate staining around somata and primary dendrites. Similar VGLUT3-ir pericellular axon terminal accumulations have been described in the neocortex and hippocampus using differently raised antibodies (Hioki et al., 2004; Somogyi et al., 2004). In frontal and horizontal sections, the VGLUT3-ir PBs were not diffusely distributed but grossly arranged in a layer-like pattern throughout the entire rostrocaudal extent of the LS. In frontal sections, the onion skin-like distribution – which is also typical of other modulatory afferents of the LS forming PBs – was best appreciable at intermediate and caudal levels (Jakab and Leranth, 1995; Risold and Swanson, 1997a,b). The major layers and clusters of VGLUT3-ir were found in the rostral and medial LSI and in a narrow zone bordering the MS. Moreover, the entire LSD exhibited prominent VGLUT3-ir PBs thinning out in the subventricular zone of the LSI, whereas the LSV was stained by VGLUT3-ir fibers not forming as distinct PBs which is, e.g., also typical of serotonergic fibers (Dinopoulos et al., 1993; Gall and Moore, 1984). The central LSI was nearly devoid of VGLUT3-ir terminals.

4.2. Coincidence of VGLUT3-ir with markers that define major neuron populations or afferent systems of the LS

The results described above raised the question whether the VGLUT3-ir terminals attach to well-characterized neuron populations of the LS and/or coincide with the known afferent modulatory systems. Surprisingly, co-expression with other markers was only exceptionally found. In context with the existing literature, the following functional conclusions can be drawn from the multiple-labeling experiments.

In the *telencephalon*, the most prominent source of input to the LS is the hippocampus. However, these afferents primarily terminate on distal dendrites of the GABAergic medium-sized somatospiny projection neurons of the LS which are CALB-positive (Jakab and Leranth, 1995). The hippocampal afferentiation pattern is rather compatible with the moderate to intense uniform VGLUT1-labeling of the LS (Kaneko et al., 2002; Herzog et al., 2004). Our results show that in the central (or lateral) LSI – where the bulk of CALB-ir projection neurons is situated – almost no VGLUT3-ir fibers were observed–implicating even a complete spatial segregation of these afferents from hippocampal terminals. In those LS regions, where VGLUT3-ir terminals were prominent, they intermingled with VGLUT1-ir dots, but were only exceptionally co-expressed implicating complementary distribution of these transporters also in the LS. The CALB-positive projection neurons of the central LS, in addition, receive vasopressinergic afferents from the BST which synapse on distal dendritic shafts adjacent to the hippocamposeptal synaptic contacts but also on the soma of these LS cells (De Vries and

Buijs, 1983; Jakab et al., 1991; Sofroniew, 1985). However, the vasopressinergic terminals do not form as distinct pericellular baskets. Coherently, we did not find vasopressin-ir fibers that were immunoreactive for VGLUT3 (own observations, unpublished). Although the BST contains numerous VLGUT3-mRNA-positive perikarya (Herzog et al., 2004) it is less likely the source of a widespread VGLUT3-innervation of the LS as this innervation pattern is rather typical of modulatory brainstem systems (dopaminergic, serotonergic, cholinergic).

Other, spatially restricted telencephalic projections to the LS originate in the entorhinal cortex, which sends glutamatergic afferents to the GABAergic CALR-ir LS neurons and in the vertical limb of the diagonal band of Broca, which sends PARV-positive afferents (terminating basket-like) to the medioventral LSI (Harkany et al., 2003; Kiss et al., 1997; Leranth et al., 1999). Although the immunolabeling of VGLUT3 partly overlapped with the distribution patterns for PARV and CALR, no major co-localization of these markers was found. Finally, there is an extensive intrinsic arborization of the axons of GABAergic projection neurons inside the LS organized in subregional circuits (Jakab and Leranth, 1995). These fibers and potential extrinsic, GABAergic sources (Jakab and Leranth, 1990) probably cause the heavy homogeneous VGAT-ir of the LS which was – similar to VGLUT1 and VGLUT2 – only rarely co-expressed with VGLUT3-ir.

In the *diencephalon*, projections to the LS arise in the thalamus, hypothalamus and ventral pallidum (Jakab and Leranth, 1995). Existence of VGLUT3-mRNA was repeatedly reported to be absent from the thalamus, and there are some controversial descriptions for the hypothalamus and ventral pallidum (Fremeau et al., 2002; Herzog et al., 2004; Schäfer et al., 2002). The thalamic afferents are probably represented by VGLUT2-ir as all thalamic subnuclei projecting to the LS express VGLUT2-ir and -mRNA (Fremeau et al., 2001; Herzog et al., 2001; Hur and Zaborszky, 2005; Kaneko et al., 2002; Moga et al., 1995; Staiger and Nürnberger, 1989). It remains to be elucidated whether the different VGLUT2-labeling pattern, i.e. intense, homogeneous neuropil in the rostral LS *versus* VGLUT2-ir pericellular arrangements in the caudal LS account for afferents from different thalamic subnuclei or are rather a local organization principle of identical thalamic afferents. The ventral pallidum sends a rather restricted projection to the medial LSI (Groenewegen et al., 1993) and is, therefore, not a candidate for the widespread VGLUT3-innervation. Among the variety of projections from the hypothalamus to the LS, the TH-ir fibers originating in the periventricular and basolateral hypothalamus (Jakab and Leranth, 1993) did not co-express VGLUT3-ir. A variety of substance P- or methionin-enkephalin-ir neuropeptidergic fibers that are known to emanate from different hypothalamic regions did also not co-express VGLUT3-ir (own observations, unpublished).

In the *mesencephalon*, the interpeduncular nucleus (IP) displayed a high amount of VGLUT3-mRNA except in its central and lateral parts (Herzog et al., 2004; Schäfer et al., 2002). Projections from the IP originate primarily in the apical and lateral subnuclei. As their target cells seem to be confined to the ventral LS and the formation of PB-like terminals was not reported for these afferents they are probably not a candidate for the widespread VGLUT3-innervation of the LS (Groenewegen et al., 1986; Morley, 1986; Risold and Swanson, 1997b). The expression of VGLUT3-mRNA in the substantia nigra pars compacta and ventral tegmental area has been described by Fremeau et al. (2002), but was not found by others (Gras et al., 2002; Herzog et al., 2004; Schäfer et al., 2002). The TH-ir projections of the mesencephalon which form pericellular baskets intermingle with the VGLUT3-ir PBs in the LS. Sometimes TH-ir fibers and VGLUT3-ir terminals attached to the same neurons.

The most caudal sources of LS afferents originate in the *rhombencephalon* and *spinal cord*. Among the caudal regions projecting to the LS, only the dorsal (DR) and median (MR) raphe nuclei provide a prominent serotonergic input to all subnuclei of the LS. Moreover, the DR

and MR displayed a high VGLUT3-mRNA expression in the rat and all of the serotonin transporter-positive cells in the MR and DR also expressed VGLUT3. However, no co-localization of these two markers on single neurons in the LS was reported (Fremeau et al., 2002; Gras et al., 2002; Herzog et al., 2004). We found that VGLUT3- and TrpH-ir fibers considerably overlapped in the subventricular and caudoventral LS. Hence, it is possible that serotonergic projection neurons of the raphe nuclei form two chemically distinct and spatially segregated synaptic targets in the LS like it was shown *in vitro* (Fremeau et al., 2002; Schäfer et al., 2002). On the other hand, Gras and co-workers reported that numerous neurons in the dorsal raphe were VGLUT3-ir, but not serotonergic. Thus, a second possibility is a non-serotonergic glutamatergic projection from the DR to the LS (Köhler et al., 1982; Stratford and Wirtshafter, 1990). Shutoh et al. (2008) recently found VGLUT3-ir fibers in the LSD that were immunoreactive for serotonin in adult male Sprague–Dawley rats implicating that there possibly exist strain differences. The TH-ir in the LS also comprises noradrenergic fibers originating in the locus coeruleus. The distribution of TH and DBH (dopamine-β-hydroxylase-ir, DBH-ir) inside the LS is quite similar (Risold, 2004; Risold and Swanson, 1997a). However, DBH-ir fibers in the LS do not form pericellular baskets (Antonopoulos et al., 2004; Jakab and Leranth, 1995) and VGLUT3-mRNA has consistently not been detected in the locus coeruleus (Fremeau et al., 2002; Gras et al., 2002; Herzog et al., 2004).

Schäfer et al. (2002) also described VGLUT3-mRNA in the nucleus of the solitary tract, a region that obviously projects to the entire rostrocaudal extent of the lateral septum (Luiten et al., 1982). Hitherto, it is not known, which transmitter these afferents use and whether they terminate in a layer-like pattern and/or form PBs in the LS.

4.3. Coincidence of VGLUT3-ir with markers that define minor neuron populations of the LS

There are also minor subpopulations of cells in the LS whose functional role remains to be elucidated. Little is known about the cholinergic cells in the LS of the rat (Kimura et al., 1990). In the raccoon, cholinergic neurons are numerous in the LS forming a discrete neuron subpopulation with peculiar cytochemical features (Brauer et al., 1999). In the present study, co-localization with VGLUT3-ir was detected in a subpopulation of the small population of cholinergic LS cells. Concerning their homogeneous somatic VGLUT3-staining these cells resembled cholinergic interneurons in the nucleus accumbens supporting the view that the LS is morpho-functionally similar to the striatum (Alheid and Heimer, 1988; Gritti et al., 2006; Riedel et al., 2002; Risold, 2004; Swanson and Risold, 2000). Some of the ChAT-monolabeled cells were strongly immunoreactive and, thus, resembled cholinergic projection neurons in the MS (Harkany et al., 2003; Nickerson Poulin et al., 2006). Others were faintly ChAT-labeled like those in the Islands of Calleja (own observations). Taken together, the heterogeneity of this small cell population reminds of other transition zones in the basal forebrain where features of the morpho-functionally adjoining regions mix (Härtig et al., 2003; Heimer et al., 1997a,b; Swanson and Petrovich, 1998).

Finally, the LSD harbors WFA-binding perineuronal nets around neurons that are probably GABAergic (Brauer et al., 1993; Seeger et al., 1994). PNs are formations of the extracellular matrix subserving multiple functions including neuroprotection in oxidative stress (Celio et al., 1998; Morawski et al., 2004). In our samples, high VGLUT3-ir was found in the regions of WFA-binding, however, only few cells were coated with PNs and outlined by VGLUT3-ir terminals at the same time indicating that different neuron populations are labeled by these markers.

In summary, VGLUT3-ir structures of the LS form PBs which are arranged in a layer-like pattern. This is typical of many other modulatory transmitter systems terminating in and/or passing the lateral septum (Jakab and Leranth, 1995). The VGLUT3-ir PBs ensheath a particular population of cells which is distinct from the well defined subpopulations. These

results indicate that an origin of VGLUT3-ir afferents from a deeper brainstem modulatory system is probable. The median and dorsal raphe nuclei are potent candidates for these VGLUT3-ir projections as they have been shown to be the origin of VGLUT3-positive projections to a variety of brain regions (Geisler et al., 2007; Hioki et al., 2004; Somogyi et al., 2004). Tract tracing studies will elucidate whether the VGLUT3-ir fibers originate in pure glutamatergic neurons or in neurons that co-produce another transmitter, but release the glutamate at different sites.

Supplementary Material

Refer to Web version on PubMed Central for supplementary material.

Acknowledgments

References

Alheid GF, Heimer L. New perspectives in basal forebrain organization of special relevance for neuropsychiatric disorders: the striatopallidal, amygdaloid, and corticopetal components of substantia innominata. Neuroscience 1988;27:1–39. [PubMed: 3059226]

Antonopoulos J, Latsari M, Dori I, Chiotelli M, Parnavelas JG, Dinopoulos A. Noradrenergic innervation of the developing and mature septal area of the rat. J Comp Neurol 2004;476:80–90. [PubMed: 15236468]

Bialowas J, Frotscher M. Choline acetyltransferase-immunoreactive neurons and terminals in the rat septal complex: a combined light and electron microscopic study. J Comp Neurol 1987;259:298–307. [PubMed: 3294933]

Brauer K, Härtig W, Bigl V, Brückner G. Distribution of parvalbumin-containing neurons and lectin-binding perineuronal nets in the rat basal forebrain. Brain Res 1993;631:167–170. [PubMed: 8298990]

Brauer K, Holzer M, Brückner G, Tremere L, Rasmusson DD, Poethke R, Arendt T, Härtig W. Two distinct populations of cholinergic neurons in the septum of raccoon (*Procyon lotor*): evidence for a separate subset in the lateral septum. J Comp Neurol 1999;412:112–122. [PubMed: 10440713]

Celio MR, Baier W, Schärer L, de Viragh PA, Gerday C. Monoclonal antibodies directed against the calcium-binding protein parvalbumin. Cell Calcium 1988;9:81–86. [PubMed: 3383226]

Celio MR, Baier W, Schärer L, Gregersen HJ, de Viragh PA, Norman AW. Monoclonal antibodies directed against the calcium-binding protein calbindin D-28k. Cell Calcium 1990;11:599–602. [PubMed: 2285928]

Celio MR, Spreafico R, De Biasi S, Vitellaro-Zuccarello L. Perineuronal nets: past and present. Trends Neurosci 1998;21:510–515. [PubMed: 9881847]

De Vries GJ, Buijs RM. The origin of the vasopressinergic and oxytocinergic innervation of the rat brain with special reference to the lateral septum. Brain Res 1983;273:307–317. [PubMed: 6311351]

Dinopoulos A, Dori I, Parnavelas JG. Serotonergic innervation of the mature and developing lateral septum of the rat: a light and electron microscopic immunocytochemical analysis. Neuroscience 1993;55:209–222. [PubMed: 8350987]

Fremeau RT Jr, Troyer MD, Pahner I, Nygaard GO, Tran CH, Reimer RJ, Bellocchio EE, Fortin D, Storm-Mathisen J, Edwards RH. The expression of vesicular glutamate transporters defines two classes of excitatory synapse. Neuron 2001;31:247–260. [PubMed: 11502256]

Fremeau RT Jr, Burman J, Qureshi T, Tran CH, Proctor J, Johnson J, Zhang H, Sulzer D, Copenhagen DR, Storm-Mathisen J, Reimer RJ, Chaudhry FA, Edwards RH. The identification of vesicular glutamate transporter 3 suggests novel modes of signaling by glutamate. Proc Natl Acad Sci U S A 2002;99:14488–14493. [PubMed: 12388773]

Fremeau RT Jr, Voglmaier S, Seal RP, Edwards RH. VGLUTs define subsets of excitatory neurons and suggest novel roles for glutamate. Trends Neurosci 2004;27:98–103. [PubMed: 15102489]

Gall C, Moore RY. Distribution of enkephalin, substance P, tyrosine hydroxylase, and 5-hydroxytryptamine immunoreactivity in the septal region of the rat. J Comp Neurol 1984;25:212–227. [PubMed: 6202728]

Geisler S, Derst C, Veh RW, Zahm DS. Glutamatergic afferents of the ventral tegmental area in the rat. J Neurosci 2007;27:5730–5743. [PubMed: 17522317]

Gras C, Herzog E, Bellenchi GC, Bernard V, Ravassard P, Pohl M, Gasnier B, Giros B, El Mestikawy S. A third vesicular glutamate transporter expressed by cholinergic and serotonergic neurons. J Neurosci 2002;22:5442–5451. [PubMed: 12097496]

Gritti I, Henny P, Galloni F, Mainville L, Mariotti M, Jones BE. Stereological estimates of the basal forebrain cell population in the rat, including neurons containing choline acetyltransferase, glutamic acid decarboxylase or phosphate-activated glutaminase and colocalizing vesicular glutamate transporters. Neuroscience 2006;143:1051–1064. [PubMed: 17084984]

Groenewegen HJ, Ahlenius S, Haber SN, Kowall NW, Nauta WJ. Cytoarchitecture, fiber connections, and some histochemical aspects of the interpeduncular nucleus in the rat. J Comp Neurol 1986;249:65–102. [PubMed: 2426312]

Groenewegen HJ, Berendse HW, Haber SN. Organization of the output of the ventral striatopallidal system in the rat: ventral pallidal efferents. Neuroscience 1993;57:113–142. [PubMed: 8278047]

Harkany T, Härtig W, Berghuis P, Dobszay MB, Zilberter Y, Edwards RH, Mackie K, Ernfors P. Complementary distribution of type 1 cannabinoid receptors and vesicular glutamate transporter 3 in basal forebrain suggests input-specific retrograde signalling by cholinergic neurons. Eur J Neurosci 2003;18:1979–1992. [PubMed: 14622230]

Härtig W, Brauer K, Brückner G. *Wisteria floribunda* agglutinin-labeled nets surround parvalbumin-containing neurons. Neuroreport 1992;3:869–872. [PubMed: 1421090]

Härtig W, Riedel A, Grosche J, Edwards RH, Fremeau RT Jr, Harkany T, Brauer K, Arendt T. Complementary distribution of vesicular glutamate transporters 1 and 2 in the nucleus accumbens of rat: relationship to calretinin-containing extrinsic innervation and calbindin-immunoreactive neurons. J Comp Neurol 2003;465:1–10. [PubMed: 12926012]

Härtig W, Stieler J, Boerema AS, Wolf J, Schmidt U, Weissfuss J, Bullmann T, Strijkstra AM, Arendt T. Hibernation model of tau phosphorylation in hamsters: selective vulnerability of cholinergic basal forebrain neurons–implications for Alzheimer's disease. Eur J Neurosci 2007;25:69–80. [PubMed: 17241268]

Haycock JW. Stimulation-dependent phosphorylation of tyrosine hydroxylase in rat corpus striatum. Brain Res Bull 1987;19:619–622. [PubMed: 2894236]

Heimer L, Alheid GF, de Olmos JS, Groenewegen HJ, Haber SN, Harlan RE, Zahm DS. The accumbens: beyond the core-shell dichotomy. J Neuropsychiatry Clin Neurosci 1997a;9:354–381. [PubMed: 9276840]

Heimer L, Harlan RE, Alheid GF, Garcia MM, de Olmos J. Substantia innominata: a notion which impedes clinical–anatomical correlations in neuropsychiatric disorders. Neuroscience 1997b;76:957–1006. [PubMed: 9027863]

Herzog E, Bellenchi GC, Gras C, Bernard V, Ravassard P, Bedet C, Gasnier B, Giros B, El Mestikawy S. The existence of a second vesicular glutamate transporter specifies subpopulations of glutamatergic neurons. J Neurosci 2001;21:1–6.

Herzog E, Gilchrist J, Gras C, Muzerelle A, Ravassard P, Giros B, Gaspar P, El Mestikawy S. Localization of VGLUT3, the vesicular glutamate transporter type 3, in the rat brain. Neuroscience 2004;123:983–1002. [PubMed: 14751290]

Hioki H, Fujiyama F, Nakamura K, Wu SX, Matsuda W, Kaneko T. Chemically specific circuit composed of vesicular glutamate transporter 3- and preprotachykinin B-producing interneurons in the rat neocortex. Cereb Cortex 2004;14:1266–1275. [PubMed: 15142960]

Hur EE, Zaborszky L. Vglut2 afferents to the medial prefrontal and primary somatosensory cortices: a combined retrograde tracing in situ hybridization. J Comp Neurol 2005;483:351–373. [PubMed: 15682395]

Jacobowitz DM, Winsky L. Immunocytochemical localization of calretinin in the forebrain of the rat. J Comp Neurol 1991;304:198–218. [PubMed: 2016417]

Jakab, RL.; Leranth, C. Septum. In: Paxinos, G., editor. The Rat Nervous System. 2nd. Academic Press; 1995. p. 405-442.

Jakab RL, Leranth C. Presence of somatostatin or neurotensin in lateral septal dopaminergic axon terminals of distinct hypothalamic and midbrain origins: convergence on the somatospiny neurons. Exp Brain Res 1993;92:420–430. [PubMed: 7681010]

Jakab RL, Leranth C. Catecholaminergic, GABAergic, and hippocamposeptal innervation of GABAergic "somatospiny" neurons in the rat lateral septal area. J Comp Neurol 1990;302:305–321. [PubMed: 1981215]

Jakab RL, Naftolin F, Leranth C. Convergent vasopressinergic and hippocampal input onto somatospiny neurons of the rat lateral septal area. Neuroscience 1991;40:413–421. [PubMed: 2027467]

Kaneko T, Fujiyama F, Hioki H. Immunohistochemical localization of candidates for vesicular glutamate transporters in the rat brain. J Comp Neurol 2002;444:39–62. [PubMed: 11835181]

Kimura H, Tago H, Akiyama H, Hersh LB, Tooyama I, McGeer PL. Choline acetyltransferase immunopositive neurons in the lateral septum. Brain Res 1990;533:165–170. [PubMed: 2085729]

Kiss J, Borhegyi Z, Csaky A, Szeiffert G, Leranth C. Parvalbumin-containing cells of the angular portion of the vertical limb terminate on calbindin-immunoreactive neurons located at the border between the lateral and medial septum of the rat. Exp Brain Res 1997;113:48–56. [PubMed: 9028774]

Kocsis K, Kiss J, Csaki A, Halasz B. Location of putative glutamatergic neurons projecting to the medial preoptic area of the rat hypothalamus. Brain Res Bull 2003;61:459–468. [PubMed: 12909290]

Köhler C, Chan-Palay V, Steinbusch H. The distribution and origin of serotonin-containing fibers in the septal area: a combined immunohistochemical and fluorescent retrograde tracing study in the rat. J Comp Neurol 1982;209:91–111. [PubMed: 6749914]

Kruger GM, Mosher JT, Bixby S, Joseph N, Iwashita T, Morrison SJ. Neural crest stem cells persist in the adult gut but undergo changes in self-renewal, neuronal subtype potential, and factor responsiveness. Neuron 2002;35:657–669. [PubMed: 12194866]

Leranth C, Carpi D, Buzsaki G, Kiss J. The entorhino-septo-supramam-millary nucleus connection in the rat: morphological basis of a feedback mechanism regulating hippocampal theta rhythm. Neuroscience 1999;88:701–718. [PubMed: 10363811]

Li ZS, Furness JB. Immunohistochemical localisation of cholinergic markers in putative intrinsic primary afferent neurons of the guinea-pig small intestine. Cell Tissue Res 1998;294:35–43. [PubMed: 9724454]

Lin W, McKinney K, Liu L, Lakhlani S, Jennes L. Distribution of vesicular glutamate transporter-2 messenger ribonucleic acid and protein in the septum-hypothalamus of the rat. Endocrinology 2003;144:662–670. [PubMed: 12538629]

Luiten PG, Kuipers F, Schuitmaker H. Organization of diencephalic and brainstem afferent projections to the lateral septum in the rat. Neurosci Lett 1982;30:211–216. [PubMed: 6180361]

McIntire SL, Reimer RJ, Schuske K, Edwards RH, Jorgensen EM. Identification and characterization of the vesicular GABA transporter. Nature 1997;389:870–876. [PubMed: 9349821]

Moga MM, Weis RP, Moore RY. Efferent projections of the paraventricular thalamic nucleus in the rat. J Comp Neurol 1995;359:221–238. [PubMed: 7499526]

Montana V, Ni Y, Sunjara V, Parpura V. Vesicular glutamate transporter-dependent glutamate release from astrocytes. J Neurosci 2004;24:2633–2642. [PubMed: 15028755]

Morley BJ. The interpeduncular nucleus. Int Rev Neurobiol 1986;28:157–182. [PubMed: 2433243]

Morawski M, Brückner MK, Riederer P, Brückner G, Arendt T. Perineuronal nets potentially protect against oxidative stress. Exp Neurol 2004;188:309–315. [PubMed: 15246831]

Mullen RJ, Buck CR, Smith AM. NeuN, a neuronal specific nuclear protein in vertebrates. Development 1992;116:201–211. [PubMed: 1483388]

Nickerson Poulin A, Guerci A, El Mestikaway S, Semba K. Vesicular glutamate transporter 3 immunoreactivity is present in cholinergic basal forebrain neurons projecting to the basolateral amygdala in rat. J Comp Neurol 2006;498:690–711. [PubMed: 16917846]

Paxinos, G.; Kus, L.; Ashwell, KW.; Watson, W. Chemoarchitectonic Atlas of the Rat Forebrain. 1st. Academic press; 1998.

Paxinos, G.; Watson, W. The Rat Brain in Stereotaxic Coordinates. 4th. Academic Press; 1998.

Riedel A, Härtig W, Seeger G, Gärtner U, Brauer K, Arendt T. Principles of rat subcortical forebrain organization: a study using histological techniques and multiple fluorescence labeling. J Chem Neuroanat 2002;23:75–104. [PubMed: 11841914]

Risold, PY. The septal region. In: Paxinos, G., editor. The Rat Nervous System. 3rd. Elsevier; 2004. p. 605-632.

Risold PY, Swanson LW. Chemoarchitecture of the rat lateral septal nucleus. Brain Res Brain Res Rev 1997a;24:91–113. [PubMed: 9385453]

Risold PY, Swanson LW. Connections of the rat lateral septal complex. Brain Res Brain Res Rev 1997b; 24:115–195. [PubMed: 9385454]

Schäfer MK, Varoqui H, Defamie N, Weihe E, Erickson JD. Molecular cloning and functional identification of mouse vesicular glutamate transporter 3 and its expression in subsets of novel excitatory neurons. J Biol Chem 2002;277:50734–50748. [PubMed: 12384506]

Schwaller B, Buchwald P, Blümcke I, Celio MR, Hunziker W. Characterization of a polyclonal antiserum against the purified human recombinant calcium binding protein calretinin. Cell Calcium 1993;14:639–648. [PubMed: 8242719]

Seal RP, Edwards RH. The diverse roles of vesicular glutamate transporter 3. Handb Exp Pharmacol 2006;175:137–150. [PubMed: 16722234]

Seeger G, Brauer K, Härtig W, Brückner G. Mapping of perineuronal nets in the rat brain stained by colloidal iron hydroxide histochemistry and lectin cytochemistry. Neuroscience 1994;58:371–388. [PubMed: 7512240]

Seifert U, Härtig W, Grosche J, Brückner G, Riedel A, Brauer K. Axonal expression sites of tyrosine hydroxylase, calretinin- and calbindin-immunoreactivity in striato-pallidal and septal nuclei of the rat brain a double-immunolabeling study. Brain Res 1998;795:227–246. [PubMed: 9622641]

Sheehan TP, Chambers RA, Russell DS. Regulation of affect by the lateral septum: implications for neuropsychiatry. Brain Res Brain Res Rev 2004;46:71–117. [PubMed: 15297155]

Shutoh F, Ina A, Yoshida S, Konno J, Hisano S. Two distinct subtypes of serotonergic fibers classified by co-expression with vesicular glutamate transporter 3 in rat forebrain. Neurosci Lett 2008;432:132–136. [PubMed: 18222609]

Sofroniew, MV. Vasopressin, oxytocin and their related neurophysins. In: Björklund, A.; Hökfelt, T., editors. Handbook of Chemical Neuroanatomy: GABA and the Neuropeptides in the CNS. Vol. 4. Elsevier; 1985. p. 93-165.

Somogyi J, Baude A, Omori Y, Shimizu H, El Mestikawy S, Fukaya M, Shigemoto R, Watanabe M, Somogyi P. GABAergic basket cells expressing cholecystokinin contain vesicular glutamate transporter type 3 (VGLUT3) in their synaptic terminals in hippocampus and isocortex of the rat. Eur J Neurosci 2004;19:552–569. [PubMed: 14984406]

Staiger JF, Nürnberger F. Pattern of afferents to the lateral septum in the guinea pig. Cell Tissue Res 1989;257:471–490. [PubMed: 2790932]

Stratford TR, Wirtshafter D. Ascending dopaminergic projections from the dorsal raphe nucleus in the rat. Brain Res 1990;511:173–176. [PubMed: 1970510]

Swanson LW, Petrovich GD. What is the amygdala? Trends Neurosci 1998;21:323–331. [PubMed: 9720596]

Swanson, LW.; Risold, PY. On the basic architecture of the septal region. In: Numan, R., editor. The Behavioral Neuroscience of the Septal Region. Springer; New York: 2000. p. 1-14.
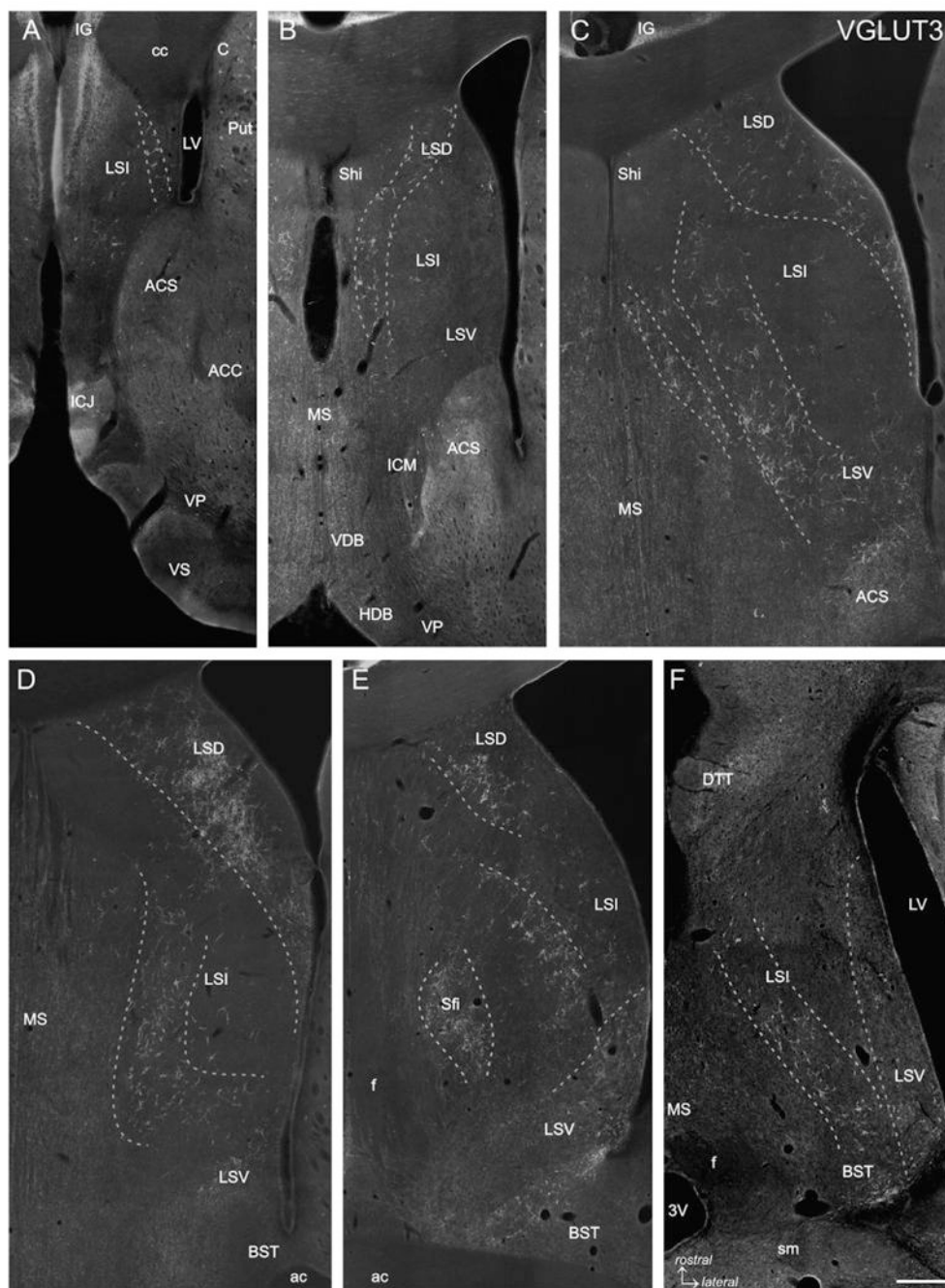
Fig. 1.
VGLUT3 immunofluorescence labeling. Five frontal sections covering the rostrocaudal extent of the lateral septum (Bregma +1.70 to −0.40 mm; A-E) and one horizontal section (Bregma −5.82 mm; Fig. 105 according to Paxinos and Watson, 1998; F) are represented. VGLUT3-ir baskets are arranged in more or less loosely arranged clusters forming oblique or curved bands which are indicated by dashed lines. In rostral and intermediate sections (A-C) VGLUT3-ir PBs occur very distinct even at low magnification, whereas in caudal sections (D and E) VGLUT3-ir PBs are less pronounced (LSD) or even absent (LSV) although a VGLUT3-ir fiber plexus is prominent. In the horizontal section (F) it is appreciable that the VGLUT3-ir PBs traversing the LSI form an oblique band from rostromedial to caudolateral, whereas the

VGLUT3-ir fibers in the LSV are most prominent at the caudal level. The caudal tips of the LSV and LSI clusters merge with the VGLUT3-ir PBs in the BST (F). 3V: third ventricle; ac: anterior commissure; ACC: accumbens nucleus, core; ACS: accumbens nucleus, shell; C: caudate nucleus; cc: corpus callosum; BST: bed nucleus of the stria terminalis; DTT: dorsal tenia tecta; f: fornix; HDB: horizontal limb of the diagonal band; ICJ: island of Calleja; ICM: insula Calleja magna; IG: indusium griseum; LSD: dorsal nucleus of the lateral septum; LSI: intermediate nucleus of the lateral septum; LSV: ventral nucleus of the lateral septum; LV: lateral ventricle; MS: medial septal nucleus; Sfi: septofimbrial nucleus; sm: stria medullaris; VDB ventral limb of the diagonal band; VP: ventral pallidum; VS: ventral striatum. Scale bar (valid for A–F) = 500 μm.
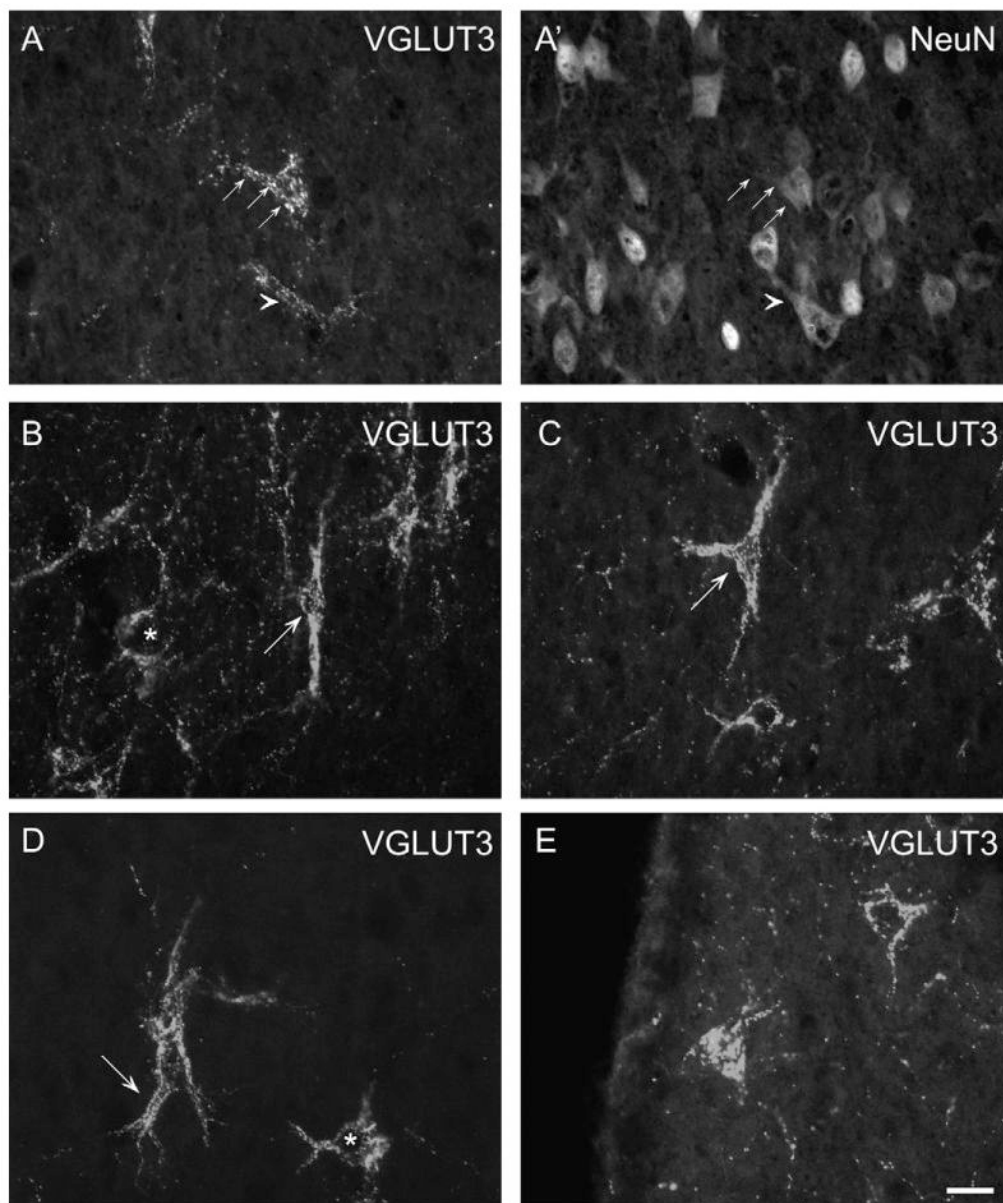
Fig. 2.
VGLUT3-NeuN immunofluorescence double labeling (A/A′): The line of arrows and the arrowhead illustrate that VGLUT-3ir PBs attach to NeuN-ir neurons. VGLUT3 single immunofluorescence labeling (B–E): The variable morphology of VGLUT3-ir pericellular baskets in the LS is illustrated. Asterisks in (B/D) indicate round somata labeled with VGLUT3-ir. In (B), an ovoid soma with bipolarly oriented primary dendrites outlined by VGLUT3-ir dots is shown (arrow). (C) Depicts a typical triangular cell (arrow) with prominent primary dendrites. In (D), the arrow points at a thick primary dendrite that trifurcates shortly after emanating from the soma. In (E), two multipolar cells are illustrated. The left seems to be cut at the surface as the entire soma area is labeled whereas the right neuron displays a VGLUT3-negative cell body outlined with VGLUT3-positive dots. Scale bar (valid for A–E) = 20 μm.
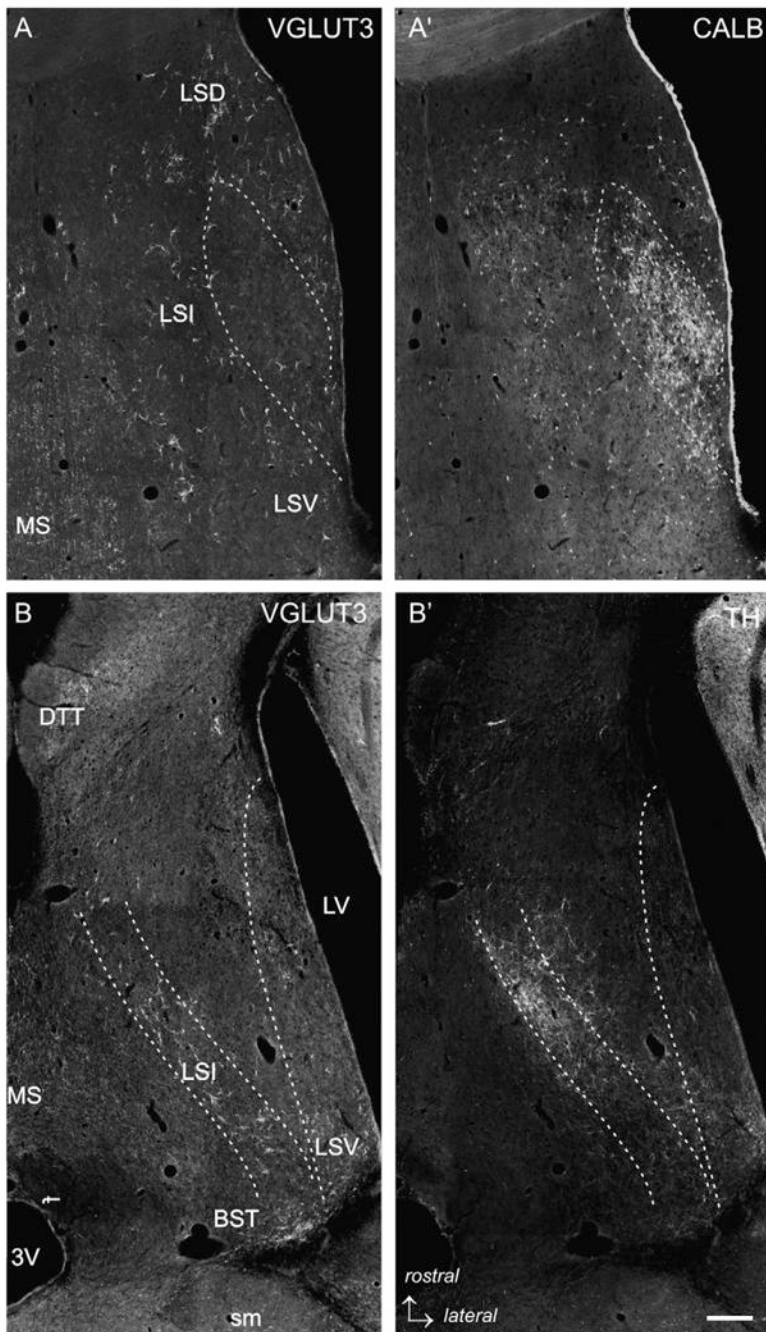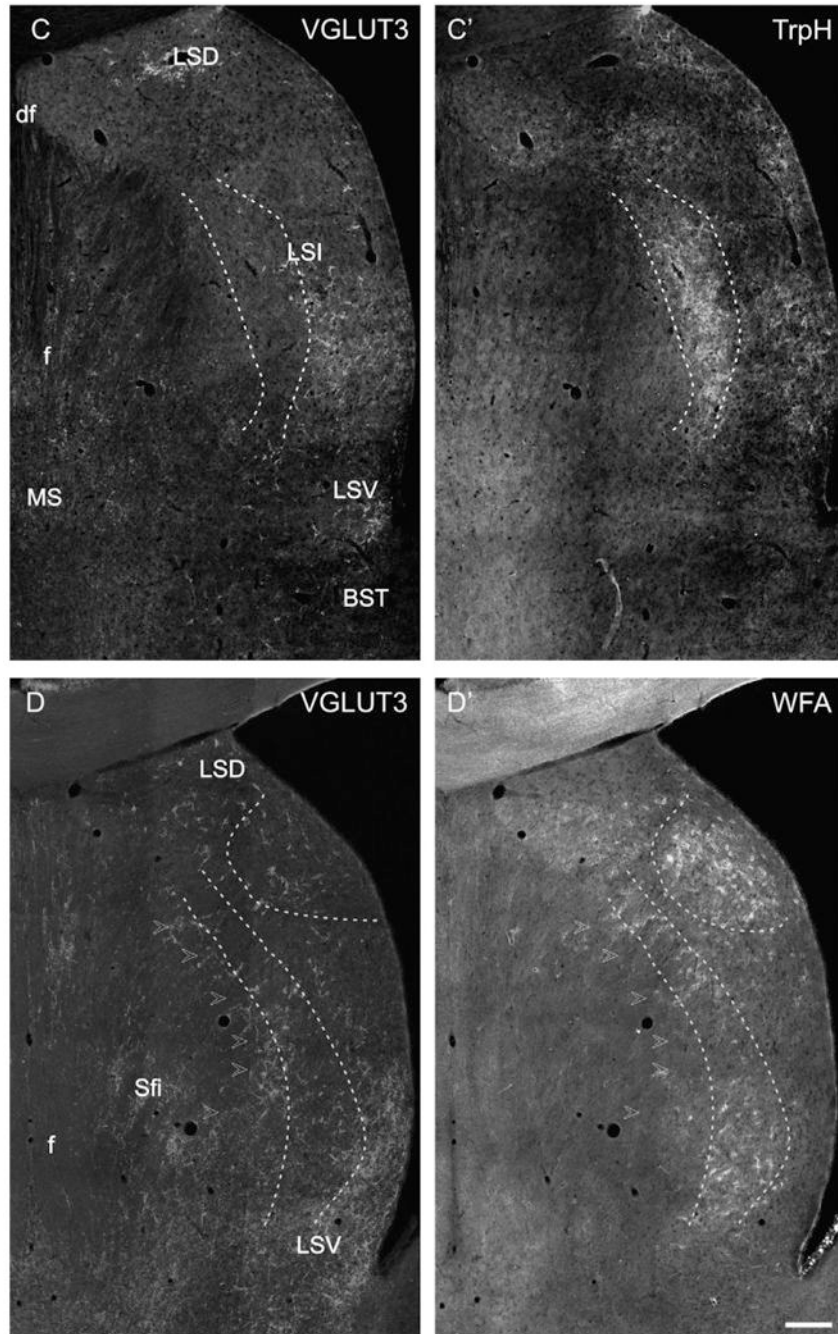
Fig. 3.
Low power photomicrographs of VGLUT3-immunofluorescence labeling with different markers. (A/A′) VGLUT3-CALB double labeling, intermediate level of the LS. The dashed lines delineate the bulk of CALB-ir projection neurons of the LS. In this region, only a few VGLUT3-ir PBs are found, whereas in the medial LSI, LSD and LSV loosely scattered CALB-ir cells intermingle with VGLUT3-ir PBs. (B/B′) VLGUT3-TH double labeling in a horizontal section of the LS (Bregma −5.82 mm according to Paxinos and Watson, 1998). It is appreciable that the TH-ir fiber network strongly overlaps with the band of VGLUT3-ir in the mediorostral but not in the laterocaudal LSI. (C/C′) VGLUT3-TrpH double labeling in a caudal section of the LS illustrating a dense cluster of TrpH-ir fibers and baskets in the medial LSI (dashed lines)

which only exceptional overlaps with VGLUT3-ir PBs. In contrast, the TrpH-ir fibers in the lateral and subventricular LSI intermingle with VGLUT3-ir. (D/D′) VGLUT3–WFA double labeling. In the caudal LS, an onion skin-like stripe that overlaps with the VGLUT3-ir band (arrowheads) of less dense WFA-staining is present. Additionally, dense WFA-binding was visible in the LSD (dashed lines). Scale bar (valid for A–D) = 500 μm.
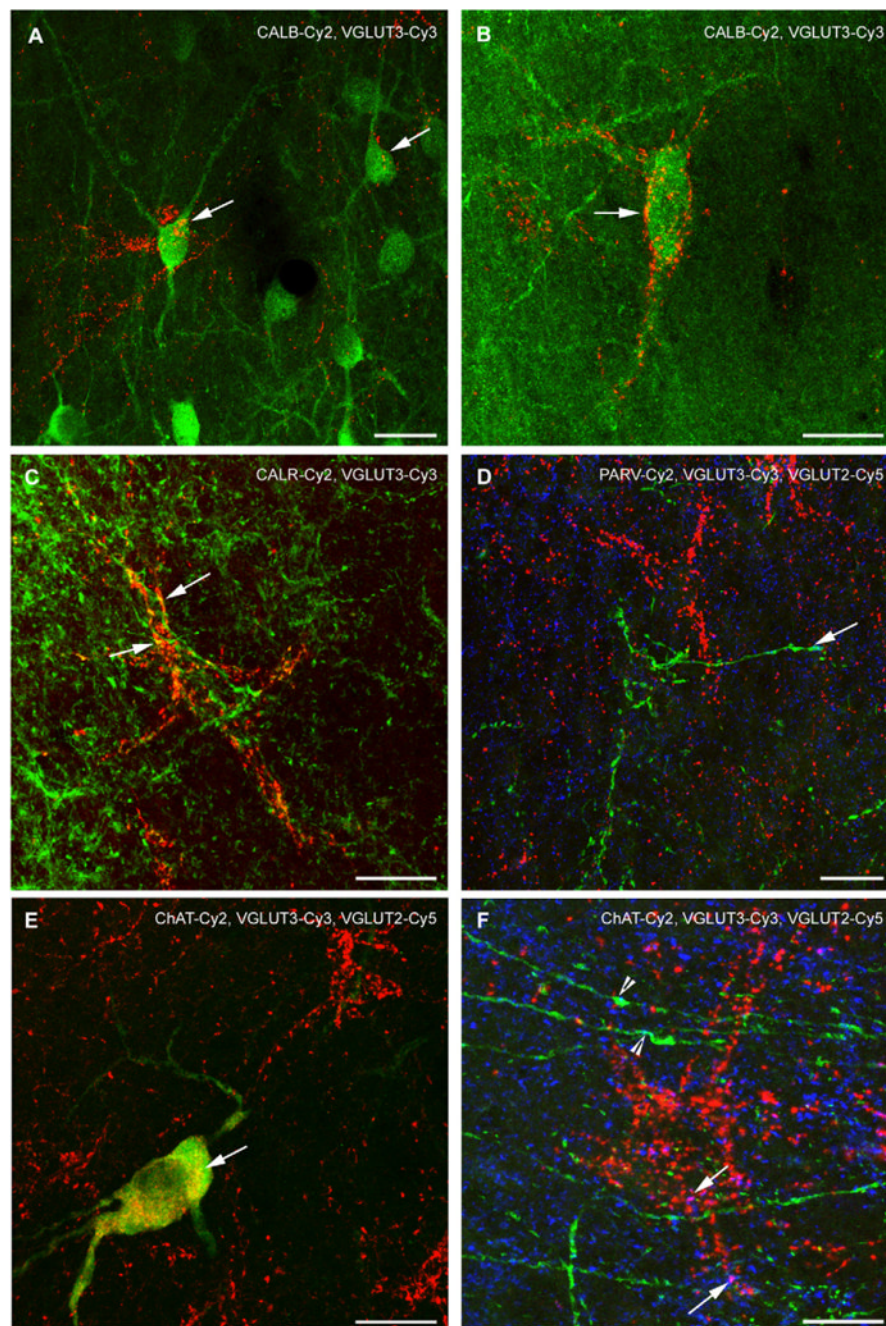
Fig. 4.
Confocal laser scanning images of VGLUT3 immunofluorescence and various simultaneously stained neuronal markers in the LS. All figures were generated from stacks of single plane images. In (A), CALB-ir cells in the subventricular LS are shown. Most of them are not labeled for VGLUT3 although immunosignals for both markers are intermingled. Note that VGLUT3-ir terminals cross two of the cells (arrows). Yellow spots are rarely found, they are a product of the z-stack projection. (B) Illustrates a CALB-ir cells in the rostral LS that is outlined by a VGLUT3-ir PB (arrow). Yellow-colored spots are a result of the z-stack projection. (C) VGLUT3-ir is partly found in the CALR-ir fiber meshwork of the LSD. However, double labeling of CALR and VGLUT3 (arrows, yellow color) within a single pericellular basket was

only exceptionally found (arrows). (D) PARV-ir fibers (green) and PBs are devoid of VGLUT3-ir (red). Such PARV-ir fibers sparsely co-express VGLUT2 (arrow, turquoise color). (E) Cholinergic neuron in the medial LSI that also displays a fine VGLUT3-ir in the perinuclear region. VGLUT3-ir (red) does not label the entire cytoplasm as ChAT-ir (green) but is distributed in a rather insular-like pattern (yellow; arrow). The cholinergic cell lies inside the cluster that is rich in VGLUT3-ir PBs, but it is not ensheathed by them. In contrast, (F) demonstrates distinct cholinergic fibers without connection to a cholinergic soma that are typically found in the subcallosal LSD (green) and display no VGLUT3-ir (red), but occasionally co-localize VGLUT2 (turquoise colored, arrowheads). Arrows indicate magenta colored, VGLUT3- and VGLUT2-co-expressing axonal endings. Scale bars = 20 μm.
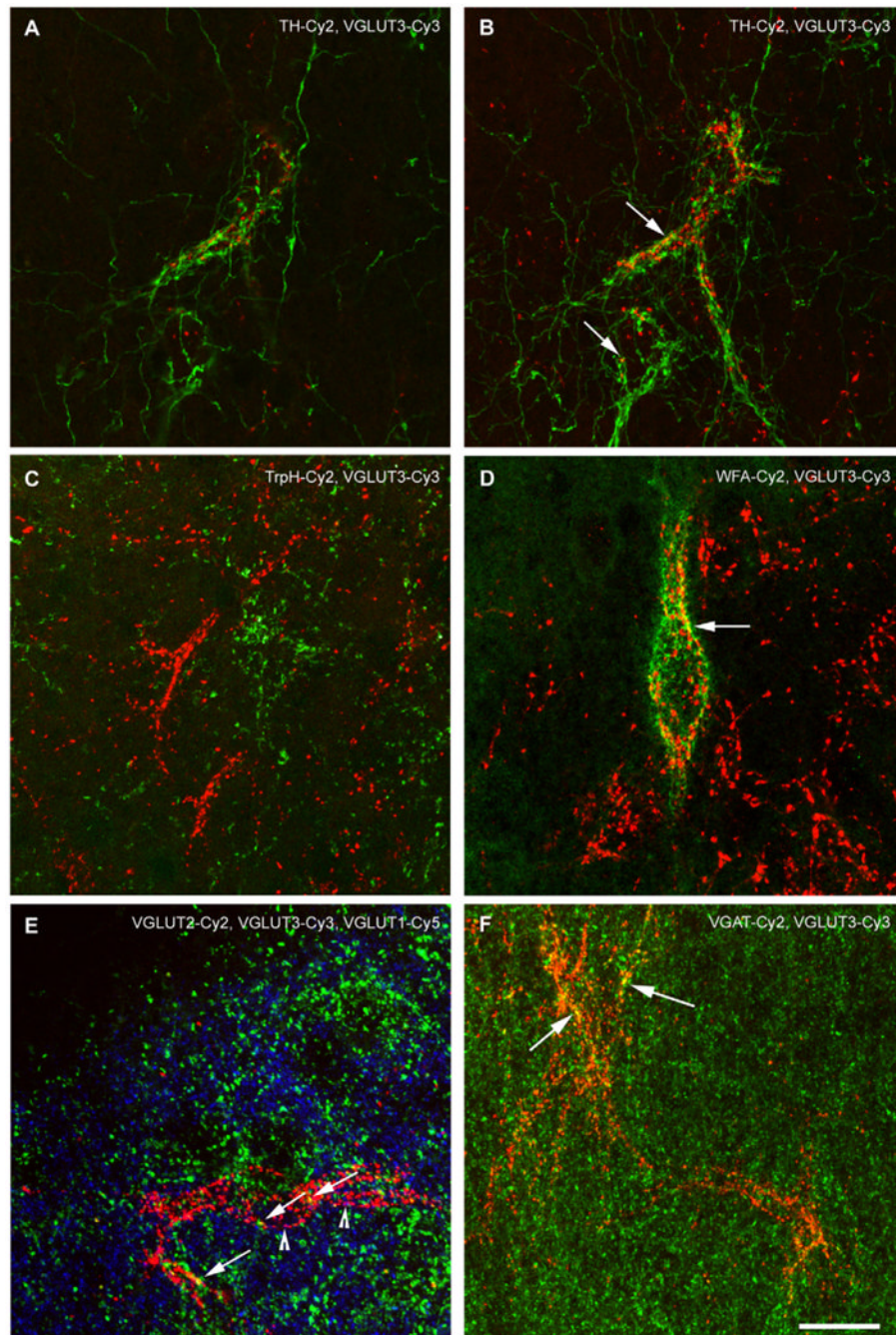
Fig. 5.
Confocal laser scanning images of VGLUT3 immunofluorescence and various co-stained neuronal markers in the LS. All images, except (A) are z-stack projections. In (A), a single confocal plane of a TH/VGLUT3-staining in the LSI is shown. It is appreciable that both markers label pericellular formations on the same neuron in different manner. TH-ir fibers are very fine and sparsely exhibit varicosities along their course. They form a dense network along the surface of the enwrapped cell displaying distinct varicosities along the presumed membrane and throughout its broader proximity. In contrast, VGLUT3-ir PBs are composed of prominent distinct dots that are obviously not connected to each other along the surface of the attached cell which is also appreciable in the other confocal images. Co-expression of TH- and

VGLUT3-ir is not found. (B) Illustrates an image stack of the cell shown in (A). A few yellow spots result from the z-stack projection (arrows), but analysis of the single planes did not reveal co-expression of VGLUT3 and TH (compare to A). (C) TrpH-ir (green) and VGLUT3-ir (red) fibers are intermingled, but spatially separated inside the LSV. (D) In the LSD, VGLUT3-ir terminals forming PBs only occasionally attach to the same cells that are ensheathed by WFA-binding perineuronal nets (green). However, the yellow merge color (arrow) resulting from the z-stacking cannot be a genuine co-localization (as seen in single z-stack planes) as components of perineuronal nets cover a pericellular space around but different from that of axonal terminals. (E) Triple labeling of vesicular glutamate transporters in the LSD revealed only rare co-localization. A VGLUT3-ir PB (red) is appreciable in-between loosely arranged VGLUT1- and VGLUT2-ir spots. Arrowheads indicate co-labeling of VGLUT3 and VGLUT1 (magenta), arrows point at VGLUT3-ir terminals that co-express VGLUT2 (yellow). Very sparse VGLUT1-/VGLUT2 double labeling is recognizable (turquoise colored, not otherwise indicated). (F) VGAT-ir (green) rarely co-localizes (yellow dots, arrows) with VGLUT3-ir (red) inside the PBs. Scale bars = 20 μm.

Table 1

List of primary antibodies and experiments

Marker	Experiment										Host species	Immunogen	Dilution	Source	References
	1	2	3	4	5	6	7	8	9	10					
NeuN	+										Mouse	Purified cell nuclei, clone A60	1:50	Chemicon/Millipore, Temecula, CA (MAB 377)	Mullen et al. (1992)
Calbindin		+									Mouse	Chicken gut calbindin-D28k	1:200	Swant, Bellinzona, Switzerland (clone CL-300)	Celio et al. (1990)
Calretinin			+								Rabbit	Human recombinant protein	1:300	Swant (serum 7699/4)	Schwaller et al. (1993)
Choline acetyltransferase				+							Goat	Human placental enzyme	1:25–1:50	Chemicon/Millipore (AB144P)	Li and Furness (1998)
Parvalbumin					+						Mouse	Carp muscle protein	1:250	Swant (clone PA-235)	Celio et al. (1988)
Tyrosine hydroxylase					+	+					Rabbit	Denatured enzyme from rat	1:100	Chemicon/Millipore (AB152)	Haycock (1987)
Tryptophan hydroxylase							+				Sheep	Recombinant rabbit enzyme pheochromocytoma	1:200	Chemicon/Millipore (AB1541)	Kruger et al. (2002)
VGLUT1								+			Mouse	GST fusion protein containing amino acids 523–560 of rat VGLUT1	1:50	Synaptic Systems, Göttingen, Germany (clone F123;135001)	Montana et al. (2004)
VGLUT2									+		Rabbit	GST fusion protein containing amino acids 510–582 of rat VGLUT2	1:250	Synaptic Systems (135102)	Montana et al. (2004)
VGLUT3	+	+	+	+	+	+	+	+	+	+	Guinea pig	GST fusion protein containing amino acids 530–588 of rat VGLUT3	1:300	Dr. R.H. Edwards, San Francisco, CA	Harkany et al. (2003)
VGAT										+	Rabbit	Synthetic peptide (amino acids 75–87 in rat)	1:250	Synaptic Systems (131002)	Härtig et al. (2007)